Collective modes of low-dimensional superfluid Fermi gases in the BCS-BEC crossover: Time-dependent variational analysis

Yu Zhou and Guoxiang Huang*
Department of Physics and Institute of Theoretical Physics, East China Normal University, Shanghai 200062, China
(Received 30 September 2006; published 12 February 2007)

We investigate collective modes and free expansions of quasi-one- and quasi-two-dimensional (Q1D and Q2D) ultracold Fermi gases in the crossover from a Bardeen-Cooper-Schrieffer (BCS) superfluid to a Bose-Einstein condensate (BEC). We solve a superfluid order parameter equation valid for the BCS-BEC crossover by employing a time-dependent variational method. We take a trial wave function of hybrid Gaussian-parabolic type, which not only reflects the low-dimensional character of the system but also allows an essentially analytical approach for the problem. We present Q1D and Q2D criteria that are valid in various superfluid regimes and show clearly the relation between the maximum condensed particle number and the parameters of the trapping potential as well as the atom-atom interaction. We demonstrate that, due to the small particle number in Q1D and Q2D condensates, the contribution to oscillating frequencies of collective modes by the quantum pressure in the strong-confinement direction is significant and hence the Thomas-Fermi approximation cannot be used. We also show that the free expansion of Q1D and Q2D superfluid Fermi gases in the strong-confinement direction is much faster than that in the weak-confinement direction.

DOI: 10.1103/PhysRevA.75.023611 PACS number(s): 03.75.Kk, 03.75.Ss, 67.40.Db

I. INTRODUCTION

The study of dimensional crossover is an important research field because the properties of phase transition and the nature of associated elementary excitations depend crucially on spatial degrees of freedom. After the remarkable experimental realization of Bose-Einstein condensation (BEC) in dilute Bose gases [1], much effort has been paid to collective excitations and dimensional crossover effects in quasi-one-dimensional (Q1D) and quasi-two-dimensional (Q2D) BECs [2–7].

Another important problem in condensed matter physics is the crossover from a BEC to a Bardeen-Cooper-Schrieffer (BCS) superfluid [8]. Since the first experimental realization of the quantum-degenerate Fermi gas in a trap [9], in recent years much interest has been focused on the study of ultracold fermionic atoms and fermionic superfluidity [10–13]. Since for dilute atomic systems the atom-atom interaction, characterized by s-wave scattering length a_s, can be tuned by magnetic-field-induced Feshbach resonance, one can manipulate the interaction strength over the range in a controllable way. Using this technique condensed fermionic atom pairs and the BCS-BEC crossover have been realized in a series of beautiful experiments [10–13]. At the same time, collective excitations in various superfluid regimes have also been investigated intensively [14–24]. This dramatic progress raises an important question about the role of the dimensionality effect in ultracold fermionic gases in the BCS-BEC crossover.

In a recent work, Martikainen and Törmä [25] studied a Q2D superfluid Fermi gas in BCS limit by solving numerically the Bogoliubov–de Gennes equations derived from a BCS Hamiltonian, they found a strong modification of the superfluid property due to discrete harmonic states. In the present work we consider Q1D and Q2D superfluid Fermi gases and investigate their collective modes and free expansions in the whole BCS-BEC crossover based on an order parameter equation obtained from time-dependent density-functional theory. The results presented here may be helpful for the experimental realization of low-dimensional superfluid Fermi gases. The paper is organized as follows. The next section gives a simple introduction to the order parameter equation that describes the dynamics of fermionic condensate. Variational equations for the parameters of hybrid Gaussian-parabolic wave functions for Q1D and Q2D systems are derived by a time-dependent variational approach. In Sec. III we provide unified criteria for Q1D and Q2D superfluid Fermi gases, which are valid for various superfluid regimes. In Sec. IV we solve the variational equations and calculate eigenvalues and eigenfrequencies of collective modes and show that the modification to oscillating frequencies contributed by quantum pressure is significant and hence a Thomas-Fermi approximation (TFA) [19–22] cannot be used. In Sec. V we discuss free expansions of the Q1D and Q2D condensates when trapping potentials are switched off. Finally, the last section contains a discussion and a summary of our main results.

II. ORDER PARAMETER EQUATION AND DYNAMIC EQUATIONS FOR A HYBRID VARIATIONAL MODEL

A. Order parameter equation for the BCS-BEC crossover

In the ground state of a superfluid fermionic atom gas, all particles are paired, with $n/2$ being the pair density. These pairs, called condensed fermionic atom pairs, originate from two-component fermionic atom systems (i.e., ^{6}Li or ^{40}K in the present experiments [10–13]) with different internal states. By means of Feshbach resonance one can easily realize the transition from the BCS to the BEC regimes. When

*Corresponding author. Electronic address: gxhuang@phy.ecnu.edu.cn

$a_s<0$ ($a_s>0$), the system is in a BCS (BEC) regime. By defining a dimensionless quantity $\eta \equiv 1/(k_F a_s)$, where $k_F = (3\pi^2 n)^{1/3}$ is the Fermi wave number, one can distinguish several different superfluidity regimes [22,23].

(i) *BCS regime* ($\eta<-1$). In this case weakly bound Cooper pairs form below a critical temperature T_c due to the many-body effect, and the system undergoes a BCS transition when the temperature T is lower than T_c. Note that both the formation of Cooper pairs and the condensation of these pairs occur simultaneously at $T=T_c$. In particular, $\eta \ll -1$ is called the deep BCS regime.

(ii) *BEC regime* ($\eta>1$). In this regime bound molecules (called dimers) are formed by two fermionic atoms at some high temperature $T=T^*$ due to two-body interaction. These preformed fermionic atom pairs have a small size and undergo a BEC phase transition at $T=T_c$ ($\ll T^*$). When $T<T_c$, the system is in the BEC superfluid phase. The particular case $\eta \gg 1$ is called the deep BEC regime.

(iii) *BCS-BEC crossover regime* ($-1<\eta<1$). This is the regime intermediate between BCS and BEC superfluidity. The condensed fermionic atom pairs in this case have the character of both BCS Cooper pairs and BEC molecules. In particular, the point $\eta=0$ is called the unitarity limit, corresponding to $a_s \to \pm\infty$. Both theoretical and experimental studies demonstrate that the transition from the BCS to the BEC regime is smooth [8], which hints that one can study the physical properties of the system in various superfluid regimes in a unified way.

There are several theoretical approaches for the study of superfluid Fermi gases in the BCS-BEC crossover. One of them—microscopic theory (called resonance superfluid theory) based on a model Hamiltonian, which includes fermionic and bosonic degrees of freedoms and their coupling—has been proposed by several authors [28–30]. In the experiments on superfluid Fermi gases, the system is confined in a finite space by an external trapping potential [10–13]. The inhomogeneous character of the system makes a microscopic approach based on a quantized model Hamiltonian difficult. However, notice that, at very low temperature (around 10^{-8} K), low-frequency collective modes cannot decay by formation of single fermionic excitations because of the gap in their energy spectrum. Thus thermal excitations play no significant role and the system can be taken as a perfect superfluid [1]. To describe the dynamics of such zero-temperature superfluid in the trapping potential $V_{ext}(\mathbf{r})$, one can use a time-dependent density-functional theory [21–23]. The action functional $L[\psi]$ of the theory is

$$L[\psi] = \int dt\, d\mathbf{r}\, \mathcal{L}(\psi, \partial\psi/\partial t, \nabla\psi), \tag{1}$$

where ψ is the superfluid order parameter,

$$\mathcal{L} = (i\hbar/2)(\psi\, \partial\, \psi^*/\partial t - \psi^*\, \partial\, \psi/\partial t) + (\hbar^2/2m)|\nabla\psi|^2 + V_{ext}(\mathbf{r})|\psi|^2 + \varepsilon(|\psi|^2)|\psi|^2$$

is the Lagrangian density. Here ε represents the bulk energy per particle of the system, which is expressed as a function of the number density $n=|\psi|^2$ and has the relation $\varepsilon(n) = (3/5)\varepsilon_F \sigma(\eta)$, with $\varepsilon_F = \hbar^2 k_F^2/(2m)$ being the Fermi energy. Some asymptotic expressions for $\sigma(\eta)$ have been obtained by fitting the calculated data [26,27]. Interpolating these asymptotic expressions for small and large $|\eta|$ one can obtain the general formula $\sigma(\eta) = \alpha_1 - \alpha_2 \arctan[\alpha_3 \eta(\beta_1 + |\eta|)/(\beta_2 + |\eta|)]$. The fitting parameters α_j ($j=1,2,3$) and β_l ($l=1,2$) for ^{6}Li (with Feshbach-resonance magnetic field 843 G) have been given in Ref. [23]. These parameters will be used in the following calculations. Notice that, although the numerical results given below are valid only for a superfluid ^{6}Li Fermi gas, the method developed here can be applied to other superfluid Fermi gases (with different α_j and β_l).

The Euler-Lagrangian equation for ψ is obtained by minimizing the action functional (1), which leads to a generalized Gross-Pitaevskii equation [21–23]

$$i\hbar \frac{\partial}{\partial t}\psi = \left(-\frac{\hbar^2}{2m}\nabla^2 + V_{ext}(\mathbf{r}) + \mu(n)\right)\psi, \tag{2}$$

where $\mu(n)$ is the equation of state (also called the bulk chemical potential) of the system [21,23]. Different superfluid regimes can be characterized by different $\mu(n)$ in corresponding regimes. According to the Gibbs-Duhem relation one can obtain the following formula [23]:

$$\mu(n) = \frac{\partial[n\varepsilon(n)]}{\partial n} = \varepsilon_F\left(\sigma(\eta) - \frac{\eta}{5}\frac{\partial\sigma(\eta)}{\partial\eta}\right). \tag{3}$$

As a function of n, the expression of the equation of state $\mu(n)$ is complicated, which prevents us from obtaining analytical results on the dynamics of the system. A simple approach for the equation of state is to take a polytropic approximation, i.e., one assumes [19–23] $\mu(n) = \mu_0 (n/n_0)^\gamma$, where μ_0 and n_0 are the reference chemical potential and particle number density of the system, introduced here for the convenience of later calculation. It is easy to show that the effective polytropic index takes the form

$$\gamma(\eta) = [(2/3)\sigma(\eta) - (2/5)\eta\sigma'(\eta) + \eta^2\sigma''(\eta)/15]/[\sigma(\eta) - \eta\sigma'(\eta)/5].$$

There are two well-known limits for the value of the polytropic index γ. One is $\gamma=2/3$ at $\eta \to -\infty$ (BCS limit) and another one is $\gamma=1$ at $\eta \to +\infty$ (BEC limit). The polytropic approximation has the advantage of allowing one to get analytical expressions for the eigenfunctions and eigenfrequencies of collective modes [18,19,21–23] for various superfluid regimes in a unified way. In fact, it is quite accurate mathematically because γ is a slowly varying function of η [19–23].

B. Dynamic equations for the parameters in a hybrid variational model

As in most experiments [10–13], we consider a harmonic trapping potential of axial symmetry, with the form $V_{ext}(\mathbf{r}) = (m/2)\omega_\perp^2[(x^2+y^2)+\lambda^2 z^2]$. Here $\lambda = \omega_z/\omega_\perp$, with $\omega_\perp$ and ω_z being the harmonic frequencies in the radial (x, y) and axial (z) directions, respectively.

To determine the dynamics of Q1D and Q2D condensates we employ a time-dependent variational method [5,31] to solve the order parameter equation (2). The corresponding Lagrange density is

$$\mathcal{L} = \frac{i\hbar}{2}\left(\psi\frac{\partial\psi^*}{\partial t} - \psi^*\frac{\partial\psi}{\partial t}\right) + \frac{\hbar^2}{2m}|\nabla\psi|^2 + V_{ext}(\mathbf{r})|\psi|^2 + \frac{\mu_0}{n_0^\gamma(1+\gamma)}|\psi|^{2+2\gamma}. \quad (4)$$

The dynamics of the condensate will be discussed in two different cases.

1. Dynamic equations for Q1D condensate

We first consider a Q1D system, i.e., the trapping potential V_{ext} in the x and y directions is much stronger than in the z direction, $\omega_\perp \gg \omega_z$ or $\lambda \ll 1$. The condensate in this case is cigar shaped and the motion of atoms in the x and y directions is governed by the ground-state wave function of the corresponding 2D linear harmonic oscillator. The condensate wave function in the radial (axial) direction should have a Gaussian (parabolic) form and hence we choose the following hybrid trial variational wave function [5]:

$$\psi = \mathcal{A}_n\left(1 - \frac{z^2}{l_z^2}\right)^{1/2\gamma} e^{-(x^2/2l_x^2 + y^2/2l_y^2)} e^{i(\beta_x x^2 + \beta_y y^2 + \beta_z z^2)}, \quad (5)$$

where l_j and β_j $(j=x,y,z)$ are the condensate width and phase parameters. Their time evolution determines completely the dynamics of the condensate. The normalization condition $\int d\mathbf{r}\,|\psi|^2 = N$ requires

$$\mathcal{A}_n^2 = \frac{\Gamma(1/\gamma + 3/2)}{\Gamma(1/\gamma + 1)}\frac{N}{l_x l_y l_z \pi^{3/2}}, \quad (6)$$

where $\Gamma(\nu)$ is the Gamma function. Inserting the trial wave function (5) into (4) and implementing 3D spatial integration we obtain

$$\frac{L}{N} = \frac{\hbar}{2}\left(\dot\beta_x l_x^2 + \dot\beta_y l_y^2 + \frac{2\gamma}{2+3\gamma}\dot\beta_z l_z^2\right) + \frac{\hbar^2}{m}\left(\frac{1}{4l_x^2} + \frac{1}{4l_y^2} + \beta_x^2 l_x^2 + \beta_y^2 l_y^2 + \frac{2\gamma}{2+3\gamma}\beta_z^2 l_z^2\right) + \frac{m\omega_\perp^2}{4}\left((l_x^2 + l_y^2) + \frac{2\gamma}{2+3\gamma}\lambda^2 l_z^2\right) + \frac{2\mu_0}{n_0^\gamma(1+\gamma)(2+3\gamma)}\left(\frac{\Gamma(1/\gamma+3/2)}{\Gamma(1/\gamma+1)}\right)^\gamma \frac{N^\gamma}{(l_x l_y l_z \pi^{3/2})^\gamma}. \quad (7)$$

In obtaining the above equations we have omitted the quantum pressure (i.e., kinetic energy) term in the axial direction (where this term is divergent due to the sharp boundary of the condensate wave function in the hydrodynamic regime) but retained it in the radial direction (where the condensate wave function has the Gaussian shape of a noninteracting gas and hence contributes the terms $1/l_x^2$ and $1/l_y^2$) [5]. The Euler-Lagrange equations

$$\frac{d}{dt}\frac{\partial L}{\partial \dot l_j} = \frac{\partial L}{\partial l_j}, \quad \frac{d}{dt}\frac{\partial L}{\partial \dot\beta_j} = \frac{\partial L}{\partial \beta_j}, \quad (8)$$

yield the dynamic equations for the condensate widths l_j and phases β_j $(j=x,y,z)$. Then we have

$$\ddot l_j = -\omega_j^2 l_j + \frac{4\gamma\mu_0}{n_0^\gamma(1+\gamma)(2+3\gamma)\pi^{3\gamma/2}m} \times\left(\frac{\Gamma(1/\gamma+3/2)}{\Gamma(1/\gamma+1)}\right)^\gamma \frac{N^\gamma}{l_j(l_x l_y l_z)^\gamma} \times\left(1 + \frac{2+\gamma}{2\gamma}\delta_{jz}\right) + \frac{\hbar^2}{m^2 l_j^3}(1-\delta_{jz}), \quad (9)$$

where $\omega_x = \omega_y = \omega_\perp$. Defining the dimensionless time $\tau = \omega_\perp t$ and the width $d_j = l_j/a_\perp$ with $a_\perp = \sqrt{\hbar/m\omega_\perp}$ (i.e., the harmonic oscillator length in the radial direction), Eq. (9) is converted into the dimensionless form

$$\frac{d^2}{d\tau^2}d_j = -\frac{\omega_j^2}{\omega_\perp^2}d_j + \frac{\mathcal{C}_{1N}}{d_j(d_x d_y d_z)^\gamma}\left(1 + \frac{2+\gamma}{2\gamma}\delta_{jz}\right) + \frac{1}{d_j^3}(1-\delta_{jz}), \quad (10)$$

where

$$\mathcal{C}_{1N} = \frac{4\gamma\mu_0 m N^\gamma}{n_0^\gamma(1+\gamma)(2+3\gamma)\pi^{3\gamma/2}\hbar^2 a_\perp^{3\gamma-2}}\left(\frac{\Gamma(1/\gamma+3/2)}{\Gamma(1/\gamma+1)}\right)^\gamma. \quad (11)$$

The ground-state configuration of the system corresponds to the time-independent solution of Eq. (10), which can be obtained by setting $\ddot d_j = 0$ with $d_j = d_{j0}$. d_{j0} satisfies the equation

$$\frac{\omega_j^2}{\omega_\perp^2}d_{j0} = \frac{\mathcal{C}_{1N}}{d_{j0}(d_{x0}d_{y0}d_{z0})^\gamma}\left(1 + \frac{2+\gamma}{2\gamma}\delta_{jz}\right) + \frac{1}{d_{j0}^3}(1-\delta_{jz}). \quad (12)$$

2. Dynamic equations for Q2D condensate

If the trapping potential in the z direction is much stronger than in the x and y directions, i.e., $\omega_\perp \ll \omega_z$ or $\lambda \gg 1$, the condensate is disk shaped and the motion of atoms in the z direction is strongly confined. In this case the condensate is a Q2D system and hence the variational wave function in the axial (radial) direction should have a Gaussian (parabolic) form [5], i.e.,

$$\psi = \mathcal{A}_n\left(1 - \frac{x^2}{l_x^2} - \frac{y^2}{l_y^2}\right)^{1/2\gamma} e^{-z^2/2l_z^2} e^{i(\beta_x x^2 + \beta_y y^2 + \beta_z z^2)}. \quad (13)$$

The normalization condition requires

$$\mathcal{A}_n^2 = \frac{(1+\gamma)N}{\gamma l_x l_y l_z \pi^{3/2}}. \quad (14)$$

The Lagrangian of the system reads

$$\frac{L}{N}=\frac{\hbar}{2}\left(\frac{\gamma}{1+2\gamma}(\dot{\beta}_x l_x^2+\dot{\beta}_y l_y^2)+\dot{\beta}_z l_z^2\right)+\frac{\hbar^2}{m}\left(\frac{\gamma}{1+2\gamma}(\beta_x^2 l_x^2+\beta_y^2 l_y^2)+\beta_z^2 l_z^2+\frac{1}{4l_z^2}\right)+\frac{m\omega_\perp^2}{4}\left(\frac{\gamma}{1+2\gamma}(l_x^2+l_y^2)+\lambda^2 l_z^2\right)+\frac{(1+\gamma)^{\gamma-1/2}\mu_0}{\gamma^\gamma(1+2\gamma)n_0^\gamma}\frac{N^\gamma}{(l_x l_y l_z \pi^{3/2})^\gamma}, \tag{15}$$

where, with a similar approach as in the above subsection, we have retained (omitted) the quantum pressure term in the axial (radial) direction. The Euler-Lagrange equations (8) now become

$$\ddot{l}_j=-\omega_j^2 l_j+\frac{2(1+\gamma)^{\gamma-1/2}\mu_0}{\gamma^\gamma m n_0^\gamma \pi^{3\gamma/2}}\frac{N^\gamma}{l_j(l_x l_y l_z)^\gamma}\left(1-\frac{1+\gamma}{1+2\gamma}\delta_{jz}\right)+\frac{\hbar^2}{m^2 l_z^3}\delta_{jz}. \tag{16}$$

Defining $d_j=l_j/a_z$ with $a_z=\sqrt{\hbar/m\omega_z}$ (i.e., the harmonic oscillator length in the axial direction), Eq. (16) can be written as the dimensionless form

$$\frac{d^2}{d\tau^2}d_j=-\frac{\omega_j^2}{\omega_z^2}d_j+\frac{\mathcal{C}_{2N}}{d_j(d_x d_y d_z)^\gamma}\left(1-\frac{1+\gamma}{1+2\gamma}\delta_{jz}\right)+\frac{1}{d_j^3}\delta_{jz}, \tag{17}$$

with $\tau=\omega_z t$ and

$$\mathcal{C}_{2N}=\frac{2(1+\gamma)^{\gamma-1/2}\mu_0 m N^\gamma}{n_0^\gamma \gamma^\gamma \pi^{3\gamma/2}\hbar^2 a_z^{3\gamma-2}}. \tag{18}$$

To find the ground-state solution we set $d_j=d_{j0}$, since it is time independent. We obtain

$$\frac{\omega_j^2}{\omega_z^2}d_{j0}=\frac{\mathcal{C}_{2N}}{d_{j0}(d_{x0}d_{y0}d_{z0})^\gamma}\left(1-\frac{1+\gamma}{1+2\gamma}\delta_{jz}\right)+\frac{1}{d_{z0}^3}\delta_{jz}. \tag{19}$$

By eliminating d_{x0} and d_{y0} it is easy to get the equation for d_{z0} as

$$d_{z0}^4=\frac{\gamma}{1+2\gamma}(\mathcal{C}_{2N}d_{z0}^{2+\gamma})^{1/(1+\gamma)}\lambda^{-2\gamma/(1+\gamma)}+1. \tag{20}$$

The width d_{z0} is the minimum value the condensate shape can attain in the axial direction.

III. CRITERIA FOR Q1D AND Q2D SUPERFLUID FERMI GASES

Up to now Q1D and Q2D superfluid Fermi gases have not been realized experimentally. It is useful to give some theoretical criteria that are helpful for future experimental efforts. Notice that the total energy per particle E_{total} and the chemical potential μ of the system are given by $E_{total}=E_{kin}+E_{pot}+E_{int}$ and $\mu=E_{kin}+E_{pot}+(1+\gamma)E_{int}$, where E_{kin}, E_{pot}, and E_{int} are, respectively, the kinetic, potential, and interaction energy, given by the last three terms of the Lagrangian (7) and (15), respectively. By a detailed calculation we obtain

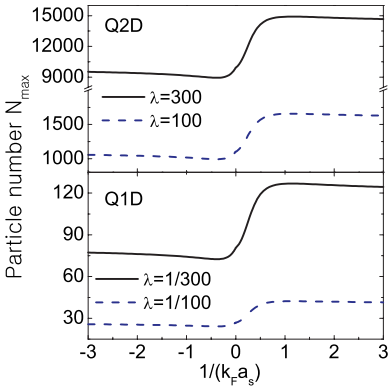

FIG. 1. (Color online) The relation between the maximum particle number N_{max} and the interaction parameter $\eta=1/(k_F a_s)$ in Q1D and Q2D superfluid Fermi gases. The trapping parameters are $\omega_z=2\pi\times 2$ Hz, $\lambda=1/300$ for Q1D and $\omega_z=2\pi\times 2100$ Hz, $\lambda=300$ for Q2D, respectively. The dashed lines show the case of $\lambda=1/100$ for Q1D and $\lambda=100$ for Q2D.

$$\mu=\begin{cases}\hbar\omega_\perp\left[1+\frac{2+3\gamma}{4\gamma}\left(\frac{2\gamma}{2+3\gamma}\mathcal{C}_{1N}^{2/\gamma}\lambda^2\right)^{\gamma/(2+\gamma)}\right] & \text{for Q1D,} \quad (21a)\\ \frac{\hbar\omega_z}{2}\left[1+\left(\frac{\mathcal{C}_{2N}}{\lambda^{(2+\gamma)/2}}\right)^{1/(1+\gamma)}\right] & \text{for Q2D.} \quad (21b)\end{cases}$$

The Q1D (Q2D) condition of the system is $\hbar\omega_z<\mu<\hbar\omega_\perp$ ($\hbar\omega_\perp<\mu<\hbar\omega_z$). From the results given by Eqs. (21) we obtain the criteria for Q1D and Q2D superfluid Fermi gases:

$$N<N_{max}=\begin{cases}\frac{1}{\mathcal{C}_1^{1/\gamma}}\left(\frac{2\gamma}{2+3\gamma}\right)^{1/\gamma}\frac{1}{\lambda} & \text{for Q1D,} \quad (22a)\\ \frac{\lambda^{(2+\gamma)/2\gamma}}{\mathcal{C}_2^{1/\gamma}} & \text{for Q2D,} \quad (22b)\end{cases}$$

where $\mathcal{C}_1=\mathcal{C}_{1N}/N^\gamma$ and $\mathcal{C}_2=\mathcal{C}_{2N}/N^\gamma$ are constants independent of N [see Eqs. (11) and (18)]. The inequalities (22a) and (22b) show clearly the constraint conditions for Q1D and Q2D superfluid Fermi gases for the particle number of the system (N), the anisotropic parameter of the trapping potential (λ), and the polytropic index of the equation of state (γ).

Based on the criteria (22a) and (22b), in Fig. 1 we have plotted the curves of maximum particle number $N=N_{max}[\gamma(\eta)]$ of the condensate for a fixed λ. In plotting the curves for the Q1D case, we have chosen $\omega_z=2\pi\times 2$ Hz for $\lambda=1/300$ (solid line) and $\lambda=1/100$ (dashed line). The curves in the Q2D case correspond to $\omega_z=2\pi\times 2100$ Hz for $\lambda=300$ (solid line) and $\lambda=100$ (dashed line). The parameter n_0 appearing in the expressions of $\mathcal{C}_{1N}$ and $\mathcal{C}_{2N}$ is chosen as the

peak density of the condensate, i.e., $n_0=n(0)=[\Gamma(1/\gamma+3/2)N]/[\Gamma(1/\gamma+1)l_{x0}l_{y0}l_{z0}\pi^{3/2}]$ for Q1D and $n_0=n(0)=(\gamma+1)N/(\gamma l_{x0}l_{y0}l_{z0}\pi^{3/2})$ for Q2D. The bulk chemical potential per particle, μ_0, is chosen as the value in the BCS limit [i.e., $\mu_0=\hbar^2(3\pi^2)^{2/3}n_0^{2/3}/(2m)$]. From the figure we see that the maximum particle number for Q1D (Q2D) in the BCS regime is less than that in the corresponding BEC regime. However, both of them have the same order of magnitude, which is around 10^2 (10^4) for given ω_z and λ. Notice that the dashed lines in the figure show the case $\lambda=1/100$ for Q1D and $\lambda=100$ for Q2D. For these λ values the maximum particle numbers allowed in Q1D and Q2D are around 10^1 and 10^3, respectively. Thus for different trapping parameters λ, the maximum particle number in the superfluid Fermi gas may be quite different. In general, as λ decreases, N_{max} increases in a way proportional to $1/\lambda$ for Q1D [see Eq. (22a)] and decreases in a way proportional to $\lambda^{(2+\gamma)/2\gamma}$ for Q2D [see Eq. (22b)]. In the BEC limit (i.e., $\gamma=1$), our theoretical result of the maximum particle number in the condensate agrees well with the experimental one reported by Görlitz *et al.* [2].

IV. COLLECTIVE MODES

Our next topic is to investigate the collective modes in Q1D and Q2D superfluid Fermi gases in the BCS-BEC crossover. Notice that, due to the axial symmetry of the trapping potential, the trial wave functions given by Eqs. (5) and (13) allow three lowest collective modes to be generated, which are the $m=2$ mode, the low-lying $m=0$ mode, and the high-lying $m=0$ mode, where m is the azimuthal angular momentum quantum number (the trivial center of mass motion is not considered). In order to get their eigenfrequencies and corresponding (linear) eigenvectors, we take $d_j=d_{j0}+\varepsilon_j(\tau)$ with the perturbation $\varepsilon_j(\tau)$ representing excitations from the ground state.

A. Excitations in Q1D

By using Eq. (12), after some algebra Eq. (10) is reduced to the following ordinary differential equations for $\varepsilon_j(\tau)$:

$$\begin{pmatrix} \ddot{\varepsilon}_x \\ \ddot{\varepsilon}_y \\ \ddot{\varepsilon}_z \end{pmatrix} = -\begin{pmatrix} \frac{(2+\gamma)\mathcal{C}_{1N}}{d_{x0}^{2+\gamma}d_{y0}^{\gamma}d_{z0}^{\gamma}}+\frac{4}{d_{x0}^{4}} & \frac{\gamma\mathcal{C}_{1N}}{d_{x0}^{1+\gamma}d_{y0}^{1+\gamma}d_{z0}^{\gamma}} & \frac{\gamma\mathcal{C}_{1N}}{d_{x0}^{1+\gamma}d_{y0}^{\gamma}d_{z0}^{1+\gamma}} \\ \frac{\gamma\mathcal{C}_{1N}}{d_{x0}^{1+\gamma}d_{y0}^{1+\gamma}d_{z0}^{\gamma}} & \frac{(2+\gamma)\mathcal{C}_{1N}}{d_{x0}^{\gamma}d_{y0}^{2+\gamma}d_{z0}^{\gamma}}+\frac{4}{d_{y0}^{4}} & \frac{\gamma\mathcal{C}_{1N}}{d_{x0}^{1+\gamma}d_{y0}^{\gamma}d_{z0}^{1+\gamma}} \\ \frac{(2+3\gamma)\mathcal{C}_{1N}}{2d_{x0}^{1+\gamma}d_{y0}^{\gamma}d_{z0}^{1+\gamma}} & \frac{(2+3\gamma)\mathcal{C}_{1N}}{2d_{x0}^{\gamma}d_{y0}^{1+\gamma}d_{z0}^{1+\gamma}} & \frac{(2+3\gamma)(2+\gamma)\mathcal{C}_{1N}}{2\gamma d_{x0}^{\gamma}d_{y0}^{\gamma}d_{z0}^{2+\gamma}} \end{pmatrix}\begin{pmatrix} \varepsilon_x \\ \varepsilon_y \\ \varepsilon_z \end{pmatrix}. \tag{23}$$

To find eigensolutions we assume $\varepsilon_j=\varepsilon_j(0)\exp(-i\omega\tau)+\text{c.c.}$ Then it is easy to get the eigenvalues of ω,

$$\omega_{\gamma K}^2=2a+4, \tag{24a}$$

$$\omega_{\gamma K_\pm}^2=(1+\gamma)a+\frac{(2+3\gamma)(2+\gamma)}{4\gamma}c+2\pm\frac{1}{2}\sqrt{R_1}, \tag{24b}$$

where we have defined $a=D\equiv\mathcal{C}_{1N}/(d_{r0}^{2+2\gamma}d_{z0}^{\gamma})$, $c=Dd_{r0}^2/d_{z0}^2$ ($d_{r0}\equiv d_{x0}=d_{y0}$), and $R_1=[2(1+\gamma)a-(2+3\gamma)(2+\gamma)c/(2\gamma)+4]^2+4\gamma(2+3\gamma)b^2$ with $b=Dd_{r0}/d_{z0}$. In the above expressions the subscripts γ and K mean that the eigenfrequencies have a dependence on the polytropic index γ and the kinetic energy (quantum pressure) in the radial direction.

With the eigenfrequencies obtained, we may calculate the corresponding eigenvectors. The normalized eigenvectors related to the eigenvalues (24a) and (24b) are found to be $(-1,1,0)$ and $(1,1,V_{\gamma K_\pm})$, respectively, with $V_{\gamma K_\pm}=[\omega_{\gamma K_\pm}^2-2(1+\gamma)a-4]/(\gamma b)$.

The collective mode with the eigenfrequency given by Eq. (24a) is the $m=2$ mode. It is a radial breathing mode because its corresponding eigenvector has only x and y components. The collective modes with the eigenfrequencies of the form Eq. (24b) are $m=0$ modes. Conventionally, the mode with the eigenfrequency $\omega_{\gamma K_+}$ ($\omega_{\gamma K_-}$) is called the high-lying (low-lying) $m=0$ mode [5]. The eigenoscillation for both the high-lying and the low-lying $m=0$ modes has three spatial components.

Notice that, if the kinetic term contributed by the quantum pressure, represented by $4/d_{r0}^4$ in Eq. (23), is disregarded, the eigenfrequencies become

$$\omega_\gamma^2=2a, \tag{25a}$$

$$\omega_{\gamma_\pm}^2=(1+\gamma)a+\frac{(2+3\gamma)(2+\gamma)}{4\gamma}c\pm\frac{1}{2}\sqrt{R_2}, \tag{25b}$$

where $R_2=[2(1+\gamma)a-(2+3\gamma)(2+\gamma)c/(2\gamma)]^2+4\gamma(2+3\gamma)b^2$. The corresponding eigenvectors are given by $(-1,1,0)$ and $(1,1,V_{\gamma_\pm})$ with $V_{\gamma_\pm}=[\omega_{\gamma_\pm}^2-2(1+\gamma)a]/(\gamma b)$.

In Fig. 2 we have shown the eigenfrequencies and the z components of the eigenvectors of the two $m=0$ modes in the Q1D superfluid Fermi gas. The left panel of the figure shows the eigenfrequencies with (solid lines) and without (dashed lines) the inclusion of the quantum pressure (kinetic energy) in x and y directions. The parameters of the system are chosen as $\omega_z=2\pi\times 2$ Hz and $\lambda=1/300$. In order to ana-

lyze the character of the motion of the two $m=0$ modes, in the right panel we have also shown the values of the z components of the corresponding eigenvectors. From the figure we can obtain the following conclusions. (i) The eigenfrequency on the BCS side is generally smaller than on the BEC side. (ii) The eigenfrequency with the inclusion of the quantum pressure in the x and y directions is larger than in the absence of the quantum pressure. (iii) The z component of the eigenvector with the quantum pressure is much less than that without the quantum pressure. (iv) The high-lying $m=0$ mode (denoted by the subscript "+") is an in-phase compressional mode along all directions (breathing mode). However, the magnitude of the z component of the eigenvectors is very small and hence it can be taken as a radial breathing mode. (v) The low-lying $m=0$ mode (denoted by the subscript "−") corresponds to axial oscillation of the condensate width which is out of phase with the oscillation along the radial direction. Note that the magnitude of the axial oscillation is much larger than that of the radial oscillation. Thus this mode can be called an axial breathing mode.

B. Excitations in Q2D

Now we consider the excitations in Q2D. Using Eqs. (17) and (19) we obtain the following equations for the perturbation $\varepsilon_j(\tau)$:

$$\begin{pmatrix} \ddot{\varepsilon}_x \\ \ddot{\varepsilon}_y \\ \ddot{\varepsilon}_z \end{pmatrix} = -\begin{pmatrix} \dfrac{(2+\gamma)\mathcal{C}_{2N}}{d_{x0}^{2+\gamma}d_{y0}^{\gamma}d_{z0}^{\gamma}} & \dfrac{\gamma\mathcal{C}_{2N}}{d_{x0}^{1+\gamma}d_{y0}^{1+\gamma}d_{z0}^{\gamma}} & \dfrac{\gamma\mathcal{C}_{2N}}{d_{x0}^{1+\gamma}d_{y0}^{\gamma}d_{z0}^{1+\gamma}} \\ \dfrac{\gamma\mathcal{C}_{2N}}{d_{x0}^{1+\gamma}d_{y0}^{1+\gamma}d_{z0}^{\gamma}} & \dfrac{(2+\gamma)\mathcal{C}_{2N}}{d_{x0}^{\gamma}d_{y0}^{2+\gamma}d_{z0}^{\gamma}} & \dfrac{\gamma\mathcal{C}_{2N}}{d_{x0}^{\gamma}d_{y0}^{1+\gamma}d_{z0}^{1+\gamma}} \\ \dfrac{\gamma^2\mathcal{C}_{2N}}{(1+2\gamma)d_{x0}^{1+\gamma}d_{y0}^{\gamma}d_{z0}^{1+\gamma}} & \dfrac{\gamma^2\mathcal{C}_{2N}}{(1+2\gamma)d_{x0}^{\gamma}d_{y0}^{1+\gamma}d_{z0}^{1+\gamma}} & \dfrac{(2+\gamma)\gamma\mathcal{C}_{2N}}{(1+2\gamma)d_{x0}^{\gamma}d_{y0}^{\gamma}d_{z0}^{2+\gamma}} + \dfrac{4}{d_{z0}^{4}} \end{pmatrix} \begin{pmatrix} \varepsilon_x \\ \varepsilon_y \\ \varepsilon_z \end{pmatrix}. \tag{26}$$

For solving the eigenvalue problem we take $\varepsilon_j(\tau) = \varepsilon_j(0)\exp(-i\omega\tau)+\text{c.c.}$ Then we obtain the eigenvalues

$$\omega_{\gamma K}^2 = 2a, \tag{27a}$$

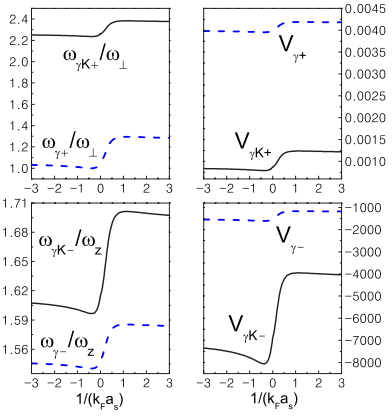

FIG. 2. (Color online) Eigenfrequencies (left panel) and the z component of the corresponding eigenvectors (right panel) of the $m=0$ modes in the Q1D superfluid Fermi gas. The solid (dashed) lines represent the case that the quantum pressure of the radial direction is (is not) included. The subscript "+" ("−") denotes the high-lying (low-lying) $m=0$ mode. The parameters are chosen as $\omega_z = 2\pi\times 2$ Hz and $\lambda = 1/300$.

$$\omega_{\gamma K_\pm}^2 = (1+\gamma)a + \frac{(2+\gamma)\gamma c}{2(1+2\gamma)} + 2\lambda^2 \pm \frac{1}{2}\sqrt{R_1}, \tag{27b}$$

where $R_1 = [2(1+\gamma)a - (2+\gamma)\gamma c/(1+2\gamma) - 4\lambda^2]^2 + 8\gamma^3 b^2/(1+2\gamma)$, and the definitions of a, b, c, and D are the same as those given in the Q1D case.

The normalized eigenvector for the $m=2$ mode [with the eigenvalue given by Eq. (27a)] is $(-1,1,0)$. This is a radial breathing mode with no oscillation in the axial (z) direction. The normalized eigenvectors with the eigenfrequencies $\omega_{\gamma K_\pm}$ are $(1,1,V_{\gamma K_\pm})$; here $V_{\gamma K_\pm} = [\omega_{\gamma K_\pm}^2 - 2(1+\gamma)a]/(\gamma b)$. Thus, as in the 1D case, the system allows two $m=0$ modes, i.e., the high-lying $m=0$ mode (represented by the subscript "+") and the low-lying $m=0$ mode (represented by the subscript "−").

Shown in Fig. 3 are the eigenfrequencies and z components of the eigenvectors of the two $m=0$ modes in Q2D. The parameters are chosen as $\omega_z = 2\pi\times 2100$ Hz and $\lambda = 300$. We see that the basic character of the eigenfrequencies is the same as in Q1D. However, the z components of the eigenvectors have different properties in comparison with the Q1D case. (i) The magnitude of the z component of the eigenvector of the high-lying $m=0$ mode is much larger than those of the x and y components and hence this mode is an axial breathing mode. (ii) The magnitude of the z component of the eigenvector of the low-lying $m=0$ mode is much smaller than those of the x and y components and hence this mode is a radial breathing mode. (iii) Contrary to the case of the Q1D, the magnitude of the z component for both $m=0$ modes with the inclusion of the quantum pressure in the strong-confining direction is larger than that in the case with-

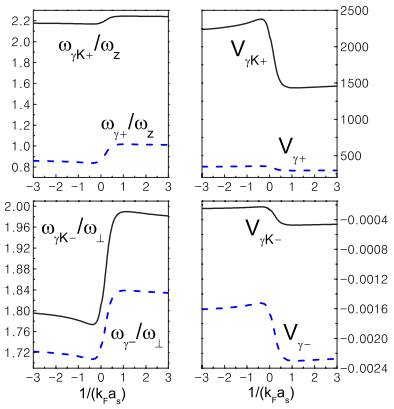

FIG. 3. (Color online) Eigenfrequencies (left panel) and the z component of the corresponding eigenvectors (right panel) of the $m=0$ modes in the Q2D superfluid Fermi gas. The solid (dashed) lines represent the case that the kinetic energy of the axial direction is (is not) included. The subscript "+" ("−") denotes the high-lying (low-lying) $m=0$ mode. The parameters are chosen as $\omega_z=2\pi\times 2100$ Hz and $\lambda=300$.

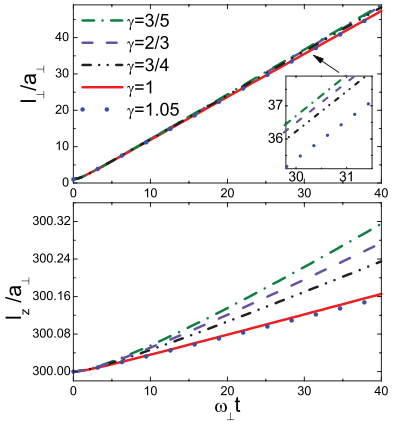

FIG. 4. (Color online) Time evolution of condensate widths of the Q1D superfluid Fermi gas after the trapping potential is switched off. The upper and lower panels show the radial width $l_\perp/a_\perp$ and axial width $l_z/a_\perp$ for different polytropic index γ, respectively. The inset is the amplification of the small region indicated in the figure.

out the inclusion of the quantum pressure. From the results obtained from both the Q1D and the Q2D cases we see that the contribution by the quantum pressure in the strong-confining directions is significant and thus the TFA cannot be used.

V. FREE EXPANSION OF Q1D AND Q2D SUPERFLUID FERMI GASES

We know that probing the free expansion is an important experimental technique for understanding the physical property of a condensate [1]. Notice that the free expansion of 3D superfluid Fermi gases was investigated recently in both experiment [32,33] and theory [34,35]. Here we provide the theoretical results on the free expansion of Q1D and Q2D superfluid Fermi gases based on the dynamical equations given above.

A. Free expansion of a Q1D superfluid Fermi gas

To study the free expansion of a Q1D condensate we start from Eq. (9) by switching off the trap, i.e., the first term on the right-hand side is set to zero. For convenience we introduce the dimensionless variables $l_\perp=a_\perp b_\perp$ and $l_z=a_z b_z$, where $a_\perp=\sqrt{\hbar/m\omega_\perp}$ and $a_z=\sqrt{2\mu/m\omega_z^2}$ are the harmonic oscillator length of the trapping potential in the x and y directions and the TF radius in the z directions, respectively. Then Eq. (9) is simplified as

$$\ddot{b}_\perp = \frac{\Delta}{b_\perp^{1+2\gamma} b_z^\gamma} + \frac{1}{b_\perp^3}, \tag{28a}$$

$$\ddot{b}_z = \frac{\Delta\epsilon^2}{b_\perp^{2\gamma} b_z^{1+\gamma}} \frac{2+3\gamma}{2\gamma}, \tag{28b}$$

where $\tau=\omega_\perp t$, $\Delta=C_{1N}(a_\perp/a_z)^\gamma$, and $\epsilon=a_\perp/a_z$.

Since an analytical solution of Eqs. (28a) and (28b) is not available we turn to solve them through a numerical simulation. The results for the time evolution of the condensate widths in the x and y directions (represented by $l_\perp/a_\perp$) and in the z direction (represented by $l_z/a_\perp$) have been presented in Fig. 4. From the figure we see that for a given polytropic index γ the free expansion of the condensate in the strongly confined x and y directions (i.e., the radial direction) is much faster than in the weakly confined z (i.e., axial) direction. For example, when $\tau=\omega_\perp t=30$, which corresponds to time $t=7.9$ ms, one has $l_\perp/a_\perp=36.5$ and $l_z/a_\perp=300.2$ in the case $\gamma=2/3$. The reason for the large radial expansion rate is that the particles have much higher kinetic energy (or quantum pressure) in the radial direction than in the axial direction. In addition, the expansion rates for both the radial and axial widths have a significant γ dependence. A smaller γ has a larger expansion rate, which means that the free expansion on the BCS side is faster than on the BEC side.

B. Free expansion of a Q2D superfluid Fermi gas

We now consider the free expansion of a Q2D Fermi gas. In this case the dynamics of the condensate is controlled by Eq. (16). After switching off the trapping potential the equation is reduced to

$$\ddot{b}_\perp = \frac{\Delta\epsilon^2}{b_\perp^{1+2\gamma} b_z^\gamma}, \tag{29a}$$

$$\ddot{b}_z = \frac{\Delta}{b_\perp^{2\gamma} b_z^{1+\gamma}} \frac{\gamma}{1+2\gamma} + \frac{1}{b_z^3}, \tag{29b}$$

where $\Delta=C_{2N}(a_z/a_\perp)^{2\gamma}$ and $\epsilon=a_z/a_\perp$. In obtaining the above equations we have defined $b_\perp=l_\perp/a_\perp$, $b_z=l_z/a_z$, where $a_\perp=\sqrt{2\mu/m\omega_\perp^2}$ and $a_z=\sqrt{\hbar/m\omega_z}$ are the TF radius in the x and y direction and the harmonic oscillator length of the trapping potential in the z direction, respectively.

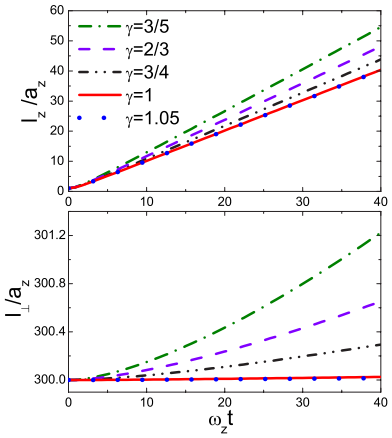

FIG. 5. (Color online) Time evolution of condensate widths of the Q2D superfluid Fermi gas after the trapping potential is switched off. The upper and lower panels show the axial width l_z/a_z and radial width $l_\perp/a_z$ for different polytropic index γ, respectively.

Shown in Fig. 5 are the numerical results of Eqs. (29a) and (29b). We see that the time evolution of the condensate widths in the z direction (represented by l_z/a_z) and in the x and y directions (represented by $l_\perp/a_z$) display very different behavior. For a given γ, the free expansion of the condensate in the strongly confined z direction is much faster than in the weakly confined x and y directions. For instance, when $\tau=\omega_z t=30$ (i.e., $t=2.3$ ms), we have $l_z/a_z=35.8$ and $l_\perp/a_z=300.4$ for $\gamma=2/3$. The giant difference of the expansion rates between the radial and the axial directions is also due to the differences between quantum pressures in different directions. As in Q1D, the expansion rates of both the axial and radial widths have a significant dependence on the polytropic index γ. The smaller γ, the larger the expansion rate.

VI. DISCUSSION AND SUMMARY

We have investigated the collective modes and free expansions of Q1D and Q2D superfluid Fermi gases in the BCS-BEC crossover. By taking hybrid trial wave functions we have solved the order parameter equation by means of a time-dependent variational method. We have provided the criteria for Q1D and Q2D superfluid Fermi gases that are valid for various superfluid regimes and display clearly the relation between the condensed particle number and the parameters of the trapping potential as well as the atom-atom interaction. We have demonstrated that, due to the small particle number in the Q1D and Q2D condensates, the contribution to oscillating frequencies by the quantum pressure in the strong-confining directions is significant and hence the Thomas-Fermi approximation cannot be used. To obtain the Q1D and Q2D superfluid Fermi gases one can use the method designed in Ref. [2] by continuously removing atoms from a highly anisotropic trap. Another way is to increase gradually the trap anisotropy from moderate to very large values while keeping the atom number fixed [5]. The results presented in this work may be useful for guiding the experimental finding of the low-dimensional superfluid Fermi gases and for understanding the physical properties of the BCS-BEC crossover.

ACKNOWLEDGMENTS

The authors thank Yong-li Ma, Wen Wen, and Xiaodong Ma for many helpful discussions. This work was supported by the NSF of China under Grants No. 10434060, No. 90403008 and No. 10674060, by the Program for Changjiang Scholars and Innovative Research Teams in Universities, and by the Key Development Program for Basic Research of China under Grant No. 2005CB724508.

[1] L. Pitaevskii and S. Stringari, *Bose-Einstein Condensation* (Clarendon Press, Oxford, 2003).
[2] A. Görlitz *et al.*, Phys. Rev. Lett. **87**, 130402 (2001); H. Moritz *et al.*, *ibid.* **91**, 250402 (2003); B. Paredes *et al.*, Nature (London) **429**, 277 (2004); D. Rychtarik *et al.*, Phys. Rev. Lett. **92**, 173003 (2004); N. L. Smith *et al.*, J. Phys. B **38**, 223 (2005); M. Kottke *et al.*, Phys. Rev. A **72**, 053631 (2005); S. Stock *et al.*, Phys. Rev. Lett. **95**, 190403 (2005).
[3] D. S. Petrov, M. Holzmann, and G. V. Shlyapnikov, Phys. Rev. Lett. **84**, 2551 (2000); D. S. Petrov, G. V. Shlyapnikov, and J. T. M. Walraven, *ibid.* **85**, 3745 (2000); I. V. Tokatly, *ibid.* **93**, 090405 (2004).
[4] C. Menotti and S. Stringari, Phys. Rev. A **66**, 043610 (2002); T.-L. Ho and M. Ma, J. Low Temp. Phys. **115**, 61 (1999).
[5] G. Hechenblaikner *et al.*, Phys. Rev. A **71**, 013604 (2005).
[6] A. Banerjee and B. Tanatar, Phys. Rev. A **72**, 053620 (2005).
[7] G. Huang, J. Szeftel, and S. Zhu, Phys. Rev. A **65**, 053605 (2002); G. Huang, V. A. Makarov, and M. G. Velarde, *ibid.* **67**, 023604 (2003); G. Huang, X.-Q. Li, and J. Szeftel, *ibid.* **69**, 065601 (2004); G. Huang, L. Deng, and C. Hang, Phys. Rev. E **72**, 036621 (2005).
[8] Q. Chen *et al.*, Phys. Rep. **412**, 1 (2005).
[9] B. DeMacro and D. S. Jin, Science **285**, 1703 (1999).
[10] S. Jochim *et al.*, Science **302**, 2101 (2003); M. Greiner, C. A. Regal, and D. S. Jin, Nature (London) **426**, 537 (2003); M. W. Zwierlein *et al.*, Phys. Rev. Lett. **91**, 250401 (2003).
[11] C. Chin *et al.*, Science **305**, 1128 (2004).
[12] C. A. Regal, M. Greiner, and D. S. Jin, Phys. Rev. Lett. **92**, 040403 (2004); M. W. Zwierlein *et al.*, *ibid.* **92**, 120403 (2004).
[13] M. W. Zwierlein *et al.*, Nature (London) **435**, 1047 (2005); Science **311**, 492 (2006); G. B. Partridge *et al.*, *ibid.* **311**, 503 (2006); M. W. Zwierlein *et al.*, Nature (London) **442**, 54 (2006); Y. Shin *et al.*, Phys. Rev. Lett. **97**, 030401 (2006).
[14] M. Bartenstein *et al.*, Phys. Rev. Lett. **92**, 203201 (2004).
[15] J. Kinast *et al.*, Phys. Rev. Lett. **92**, 150402 (2004); J. Kinast, A. Turlapov, and J. E. Thomas, Phys. Rev. A **70**, 051401(R) (2004).
[16] M. Greiner, C. A. Regal, and D. S. Jin, Phys. Rev. Lett. **94**, 070403 (2005).
[17] A. Altmeyer *et al.*, Phys. Rev. Lett. **98**, 040401 (2007).
[18] S. Stringari, Europhys. Lett. **65**, 749 (2004).

[19] H. Heiselberg, Phys. Rev. Lett. **93**, 040402 (2004); H. Hu *et al.*, *ibid.* **93**, 190403 (2004).
[20] T. K. Ghosh and K. Machida, Phys. Rev. A **73**, 013613 (2006).
[21] Y. E. Kim and A. L. Zubarev, Phys. Rev. A **70**, 033612 (2004); **72**, 011603(R) (2005).
[22] J. Yin, Y.-L. Ma, and G. Huang, Phys. Rev. A **74**, 013609 (2006).
[23] N. Manini and L. Salasnich, Phys. Rev. A **71**, 033625 (2005).
[24] R. Combescot and X. Leyronas, Phys. Rev. Lett. **93**, 138901 (2004); A. Bulgac and G. F. Bertsch, *ibid.* **94**, 070401 (2005).
[25] J.-P. Martikainen and P. Törmä, Phys. Rev. Lett. **95**, 170407 (2005).
[26] G. E. Astrakharchik *et al.*, Phys. Rev. Lett. **93**, 200404 (2004).
[27] J. Carlson *et al.*, Phys. Rev. Lett. **91**, 050401 (2003).
[28] M. Holland, J. Park, and R. Walser, Phys. Rev. Lett. **86**, 1915 (2001).
[29] Y. Ohashi and A. Griffin, Phys. Rev. Lett. **89**, 130402 (2002); Phys. Rev. A **67**, 033603 (2003); **72**, 013601 (2005).
[30] T. N. De Silva and E. J. Mueller, Phys. Rev. A **72**, 063614 (2005).
[31] V. M. Pérez-García *et al.*, Phys. Rev. Lett. **77**, 5320 (1996).
[32] K. M. O'Hara *et al.*, Science **298**, 2179 (2002).
[33] T. Bourdel *et al.*, Phys. Rev. Lett. **93**, 050401 (2004).
[34] C. Menotti, P. Pedri, and S. Stringari, Phys. Rev. Lett. **89**, 250402 (2002).
[35] G. Diana, N. Manini, and L. Salasnich, Phys. Rev. A **73**, 065601 (2006).